†***ELECTRONIC SUPPLEMENTARY MATERIAL-RSC Adv.***

Studies of molecular structure, hydrogen bonding and chemical activity of nitrofurantoin-L-proline cocrystal: A combined spectroscopic and quantum chemical approach

Jaya Pandey[1], Preeti prajapati[1], Manishkumar R. Shimpi[2], Poonam Tandon[1]*, Sitaram P. Velaga[2*], Anubha Srivastava[1] and Kirti Sinha[1]

[1]*Department of Physics, University of Lucknow, Lucknow-226007*
[2]*Luleå Technical University, Department of Health Science, S-971 87, Luleå, Sweden*

Overlapped figure of optimized structure of model I and model II using both functional B3LYP, WB97XD is given in Fig.S1. Comparison of calculated spectra of model I using functional B3LYP and WB97XD with experimental spectra of NTF-LP cocrystal and comparison of calculated spectra of both models with B3LYP functional with experimental spectra of NTF-LP cocrystal is shown in Fig.S2.Optimized structure of conformer III of NTF-LP cocrystal is shown in Fig.S3. Comparison and overlapping of the optimized structure of conformer I and conformer II is shown in Fig.S4. Fig.S5 shows the intermolecular interactions of NTF and LP with its neighboring molecules observed in bulk solid state. Comparison of experimental and calculated IR spectra of NTF is illustrated in Fig.S6. In Fig.S7 comparison of experimental and a calculated Raman spectrum of NTF is shown. Comparison of experimental and calculated IR spectra of LP is illustrated in Fig.S8. In Fig.S9 comparison of experimental and calculated Raman spectra of LP is shown. Fig.S10 shows the AIM figure of NTF whereas MEPS map of NTF is shown in Fig.S11. The comparison of HOMO-LUMO plot of NTF, LP conformer I and II of NTF-LP cocrystal with orbitals involved in electronic transitions in isolated (gaseous) phase is shown in Fig.S12. Table S1 shows the comparison of geometrical parameters of conformers I and II.. Table S2 shows the comparison of observed solid state FT-IR spectra, FT-Raman spectra and calculated harmonic vibrational wavenumbers of NTF. Comparison of FT-IR and FT-Raman spectra and calculated Vibrational wavenumbers of LP is shown in Table S3. AIM calculation to determine characteristics of hydrogen bonds and ellipticity index (ε) around bond critical point (BCP) of NTF-LP cocrystal is shown in Table S4. Table S5 shows the local reactivity descriptors of NTF molecule explaining their reactivity. The local reactivity descriptors explaining reactivity of LP molecule are shown in Table S6.

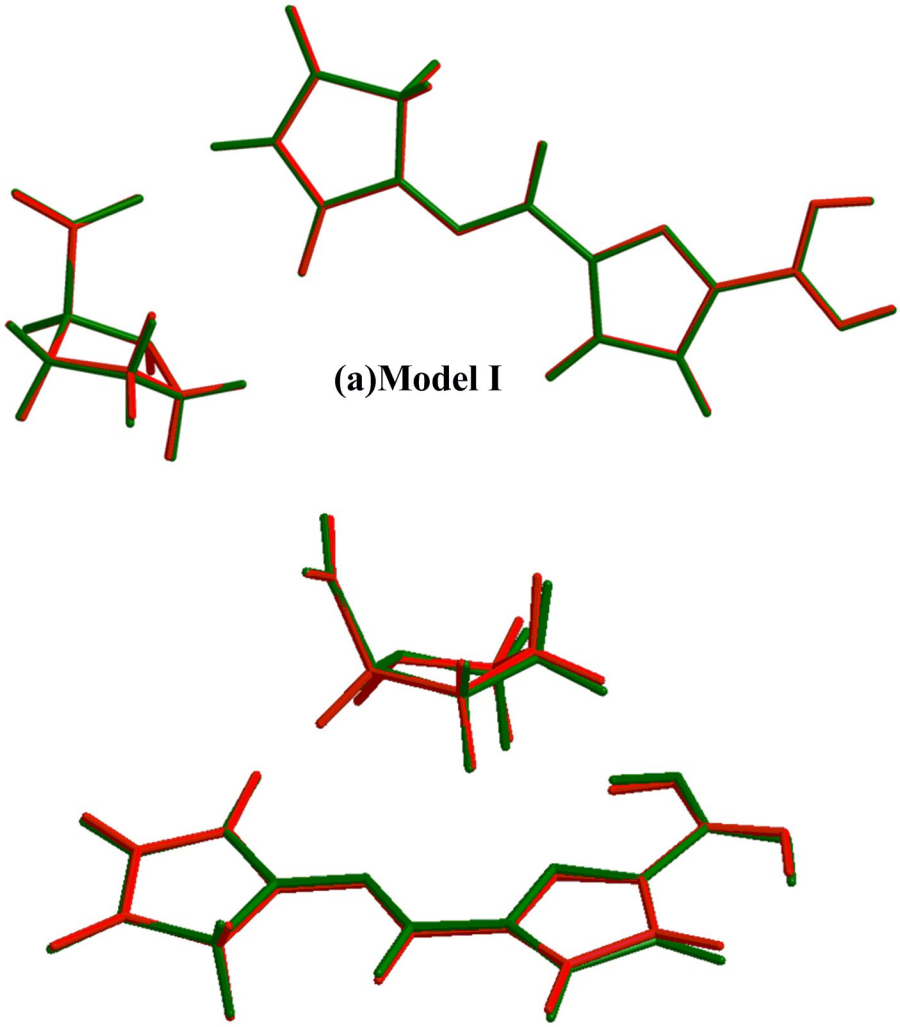

Fig.S1: (a) Overlapped figure of optimized structure of model I (a) and model II (b) using B3LYP (green) and WB97XD (red) functional.

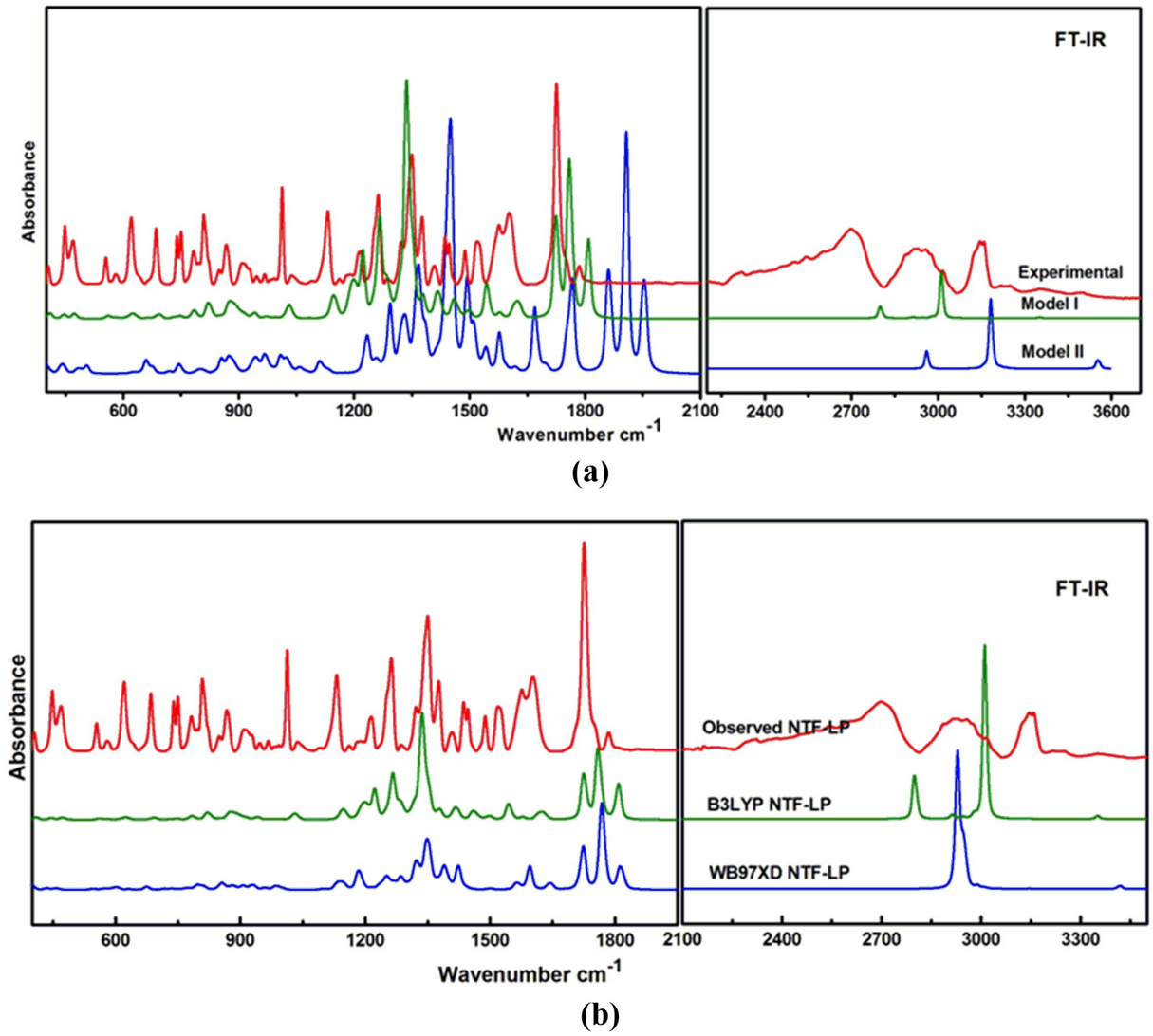

Fig.S2: (a) The comparison spectra of model I and model II using B3LYP and (b) The comparison spectra of model I and model II using B3LYP and WB97XD functional with observed spectra of NTF-LP cocrystal.

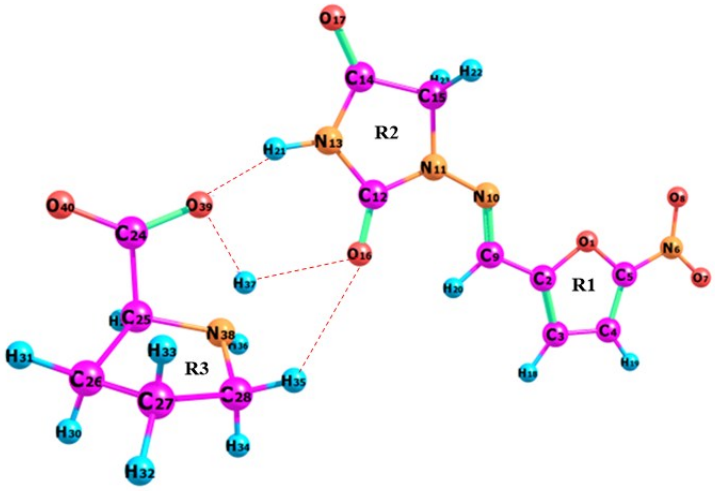

Fig.S3: Optimized structure of conformer III of NTF-LP cocrystal.

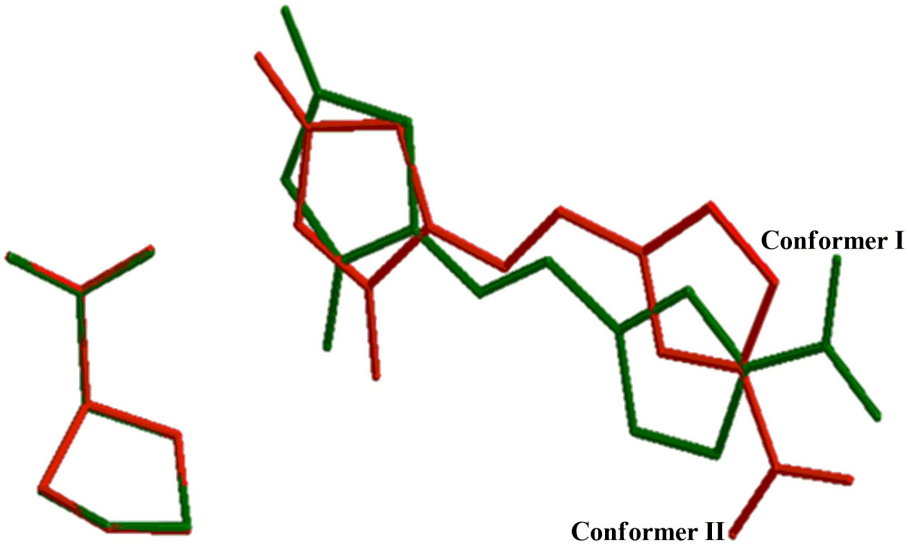

Fig.S4: Comparison of optimized structure of conformer I (green) and conformer II (red)**.**

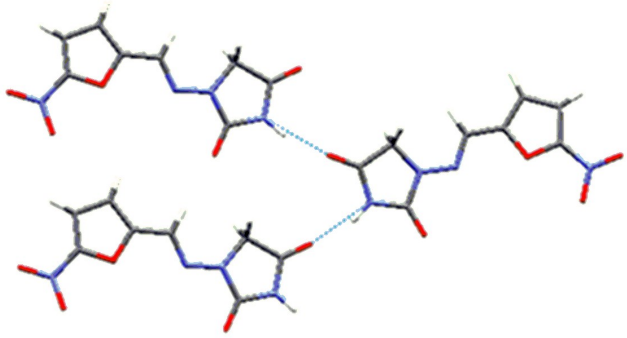

NTF interactions with neighbouring molecules

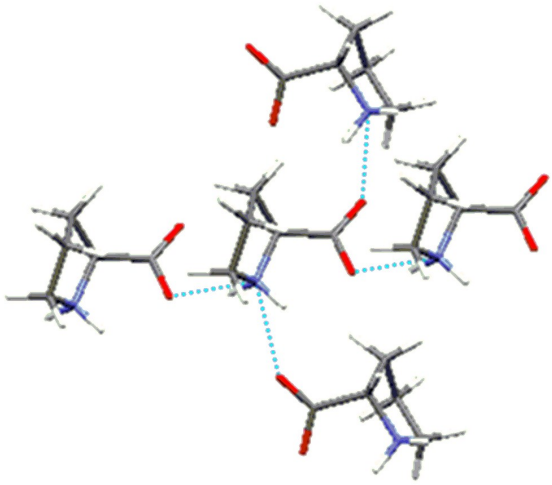

LP interactions with neighbouring molecules

Fig.S5: Intermolecular interactions of NTF and LP with their neighbouring molecules in solid state.

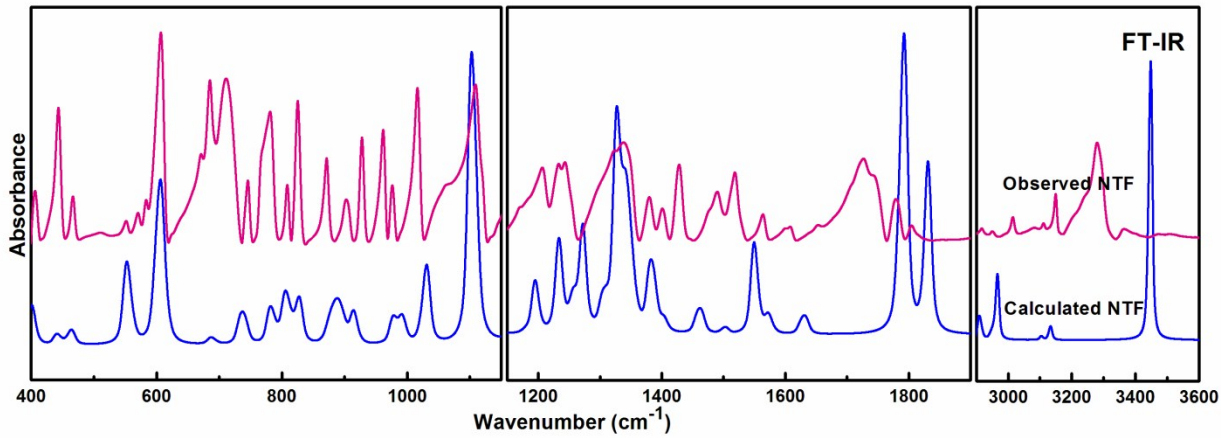

Fig.S6: Observed and calculated (scaled) FT-IR spectra of NTF in the region, 400-1150 cm^{-1}, 1150-2000 cm^{-1} and 2850-3600 cm^{-1}.

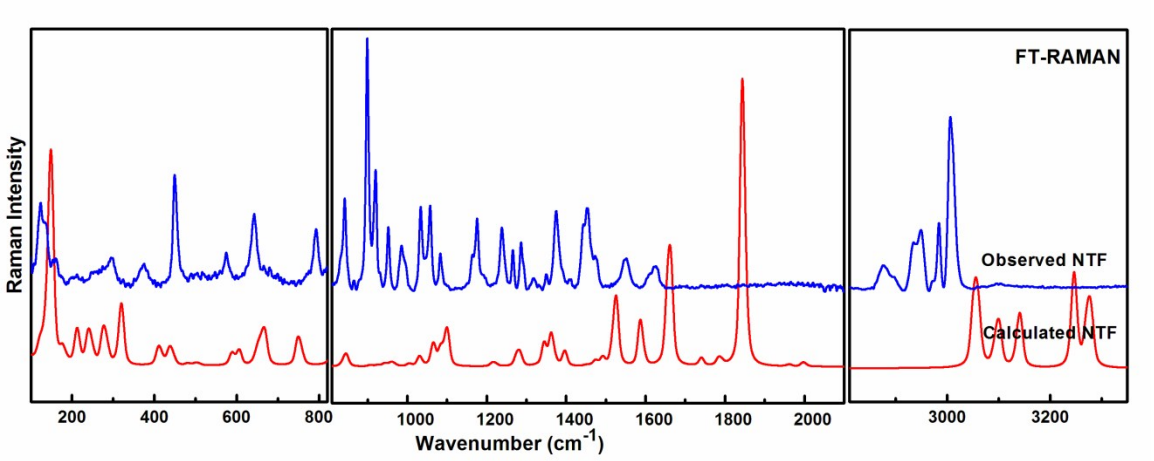

Fig.S7: Observed and calculated (scaled) FT-Raman spectra of NTF in the region, 100-800 cm^{-1}, 800-2100 cm^{-1} and 2100–3380 cm^{-1}.

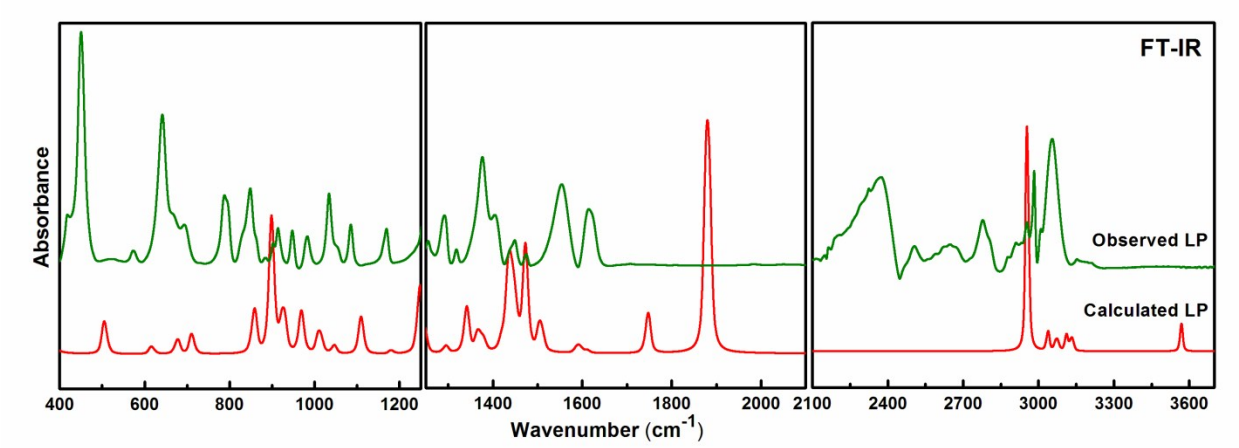

Fig.S8: Observed and calculated (scaled) FT-IR spectra of LP in the region, 400-1200 cm^{-1}, 1200-2100 cm^{-1} and 2100–3650 cm^{-1}.

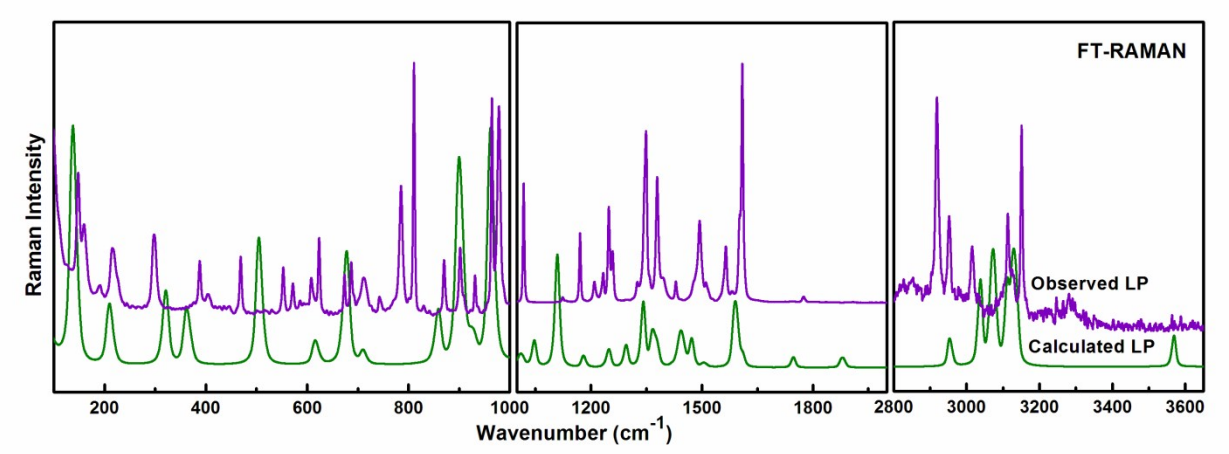

Fig.S9: Observed and calculated (scaled) FT-Raman spectra of LP in the region, 100-1000 cm^{-1}, 1000-2800 cm^{-1} and 2800–3600 cm^{-1}.

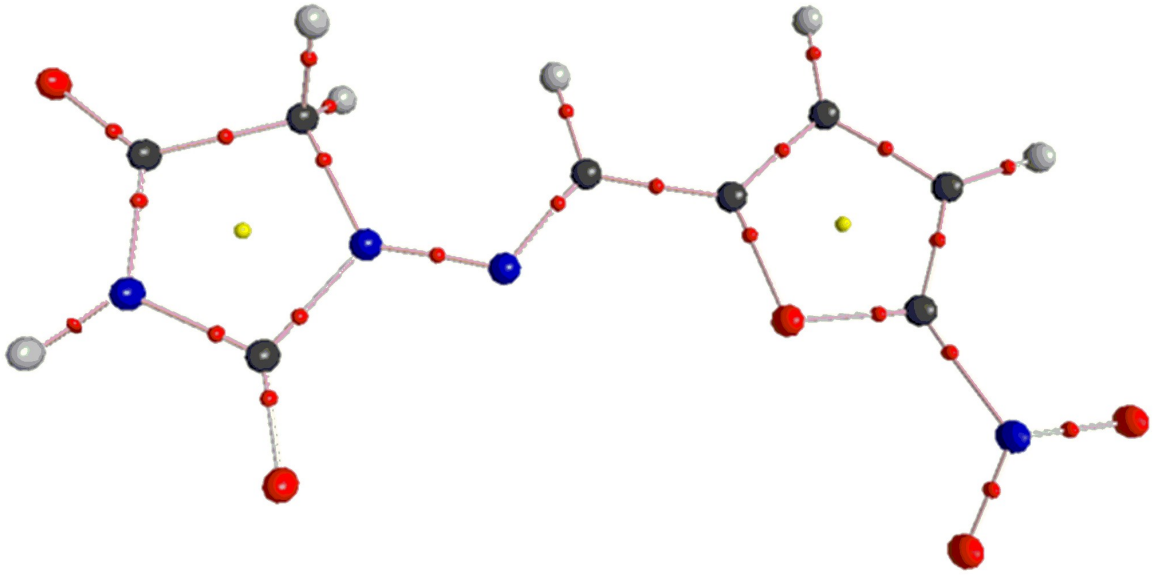

Fig.S10: Molecular graph of NTF using AIM calculation: bond path (pink lines), bond critical point (small red spheres) and ring critical points (small yellow spheres).

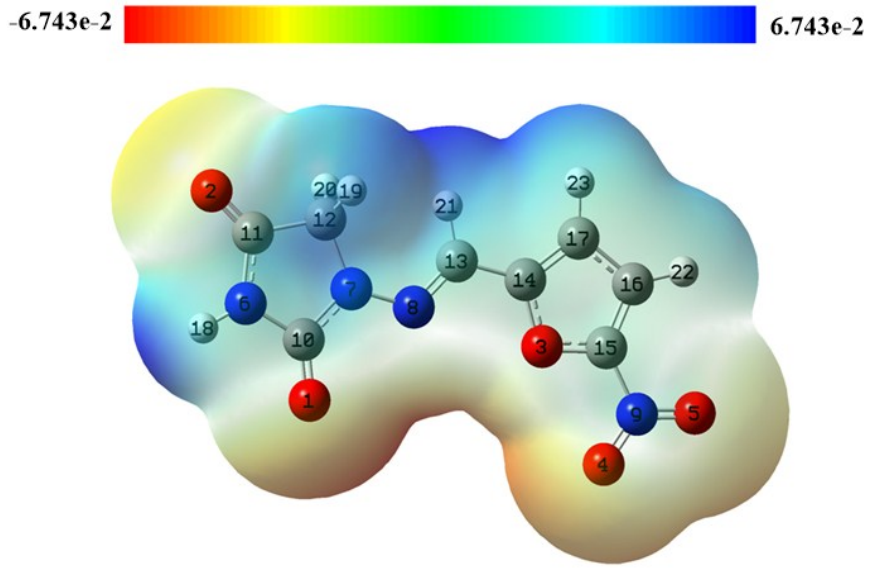

Fig.S11: Molecular electrostatic potential (MESP) mapped on iso-density surface in the range –6.743e–2 (red) to +6.743e–2 (blue) of NTF calculated at B3LYP/6-311++G(d,p) level of theory.

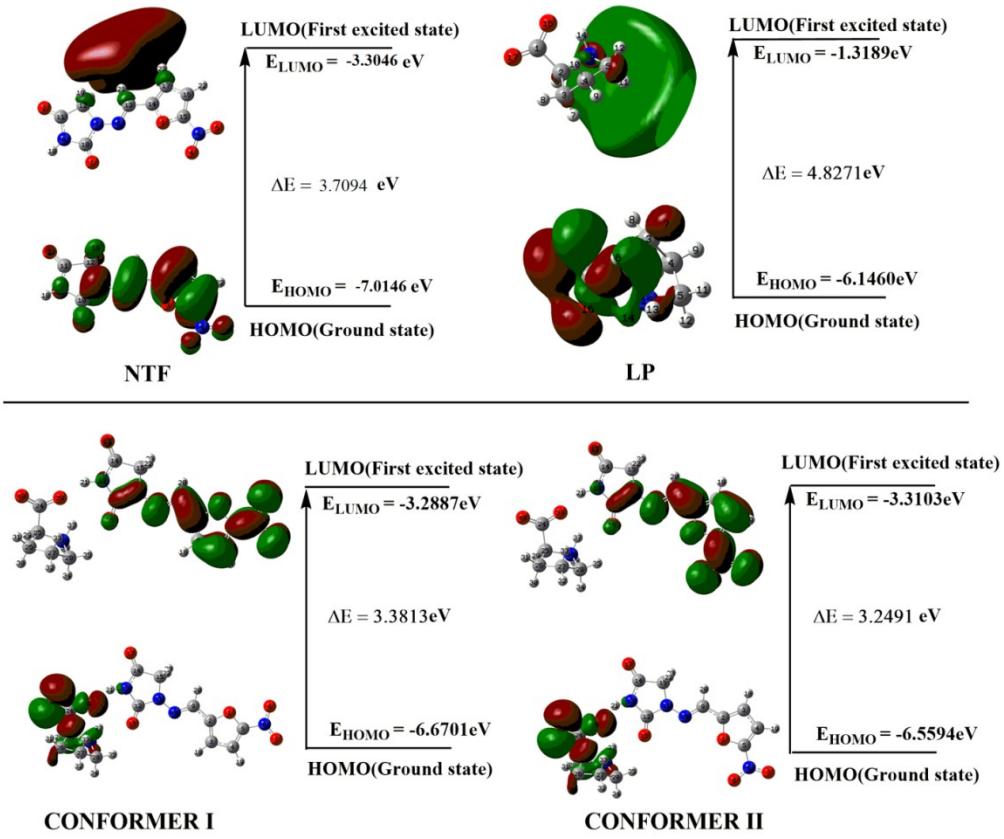

Fig.S12. HOMO-LUMO plot of NTF, LP conformer I and II of NTF-LP cocrystal with orbitals involved in electronic transitions in isolated (gaseous) phase

Table S1 Comparison of geometrical parameters, bond length, bond angle, dihedral angle for conformer I and conformer II of NTF-LP cocrystal calculated by B3LYP/6-311++G(d,p).

Parameters	Optimized conformers		Parameters	Optimized conformers	
Bond length (Å)	**I**	**II**	**Dihedral angle (°)**	**I**	**II**
O1-C2	1.364	1.359	C5-O1-C2-C3	-0.002	-0.020
O1-C5	1.350	1.350	C5-O1-C2-C9	179.983	179.878
C2-C3	1.378	1.379	C2-O1-C5-C4	0.004	0.003
C2-C9	1.443	1.442	C2-O1-C5-N6	-179.946	179.966
C3-C4	1.415	1.417	O1-C2-C3-C4	-0.001	0.029
C3-H18	1.078	1.079	O1-C2-C3-H18	-179.960	179.986
C4-C5	1.368	1.366	C9-C2-C3-C4	-179.982	-179.855
C4-H19	1.077	1.077	C9-C2-C3-H18	0.059	0.102
C5-N6	1.429	1.431	O1-C2-C9-N10	-179.797	-0.396
N6-O7	1.231	1.224	O1-C2-C9-H20	0.199	179.721
N6-O8	1.226	1.231	C3-C2-C9-N10	0.184	179.479
C9=N10	1.287	1.286	C3-C2-C9-H20	-179.821	-0.404
C9-H20	1.090	1.091	C2-C3-C4-C5	0.003	-0.026
N10-N11	1.338	1.337	C2-C3-C4-H19	179.996	179.958
N11-C12	1.403	1.404	H18-C3-C4-C5	179.961	-179.982
N11-C15	1.459	1.459	H18-C3-C4-H19	-0.047	0.002
C12-N13	1.386	1.387	C3-C4-C5-O1	-0.005	0.014
C12=O16	1.212	1.210	C3-C4-C5-N6	179.937	-179.942
N13-C14	1.379	1.378	H19-C4-C5-O1	-179.998	-179.970
N13-H21	1.039	1.039	H19-C4-C5-N6	-0.056	0.073
C14-C15	1.534	1.534	O1-C5-N6-O7	179.939	-0.158
C14=O17	1.203	1.204	O1-C5-N6-O8	-0.052	179.859
C15-H22	1.094	1.094	C4-C5-N6-O7	0.000	179.796
C15-H23	1.094	1.094	C4-C5-N6-O8	-179.991	-0.187
H21-O39	1.710	1.710	C2-C9-N10-N11	179.999	-179.934
C24-C25	1.576	1.576	H20-C9-N10-N11	0.004	-0.061
C24-O39	1.273	1.272	C9-N10-N11-C12	179.952	179.161
C24=O40	1.222	1.223	C9-N10-N11-C15	-0.020	0.258
C25-C26	1.532	1.533	N10-N11-C12-N13	179.866	-179.592
C25-H29	1.090	1.090	N10-N11-C12-O16	-0.055	0.432
C25-N38	1.525	1.524	C15-N11-C12-N13	-0.159	-0.517
C26-C27	1.538	1.538	C15-N11-C12-O16	179.921	179.507
C26-H30	1.095	1.095	N10-N11-C15-C14	-180.022	179.273
C26-H31	1.089	1.089	N10-N11-C15-H22	-61.798	-62.496
C27-C28	1.530	1.530	N10-N11-C15-H23	61.768	61.184
C27-H32	1.091	1.091	C12-N11-C15-C14	0.005	0.294
C27-H33	1.093	1.093	C12-N11-C15-H22	118.228	118.525
C28-H34	1.092	1.092	C12-N11-C15-H23	-118.205	-117.795
C28-H35	1.088	1.088	N11-C12-N13-C14	0.272	0.557
C28-N38	1.509	1.509	N11-C12-N13-H21	179.441	179.008
H36-N38	1.017	1.017	O16-C12-N13-C14	-179.809	-179.468
H37-N38	1.059	1.056	O16-C12-N13-H21	-0.639	-1.016
Bond Angle (°)					
C2-O1-C5	106.285	106.241	C12-N13-C14-C15	-0.268	-0.372
O1-C2-C3	110.026	109.996	C12-N13-C14-O17	179.743	179.620
O1-C2-C9	115.642	119.602	H21-N13-C14-C15	-179.370	-178.688
C3-C2-C9	134.332	130.403	H21-N13-C14-O17	0.641	1.304

C2-C3-C4	106.539	106.672	C12-N13-H21-O39	-4.860	-5.268
C2-C3-H18	125.485	126.078	C14-N13- H21-O39	174.190	172.957
C4-C3-H18	127.976	127.249	N13-C14-C15-N11	0.152	0.041
C3-C4-C5	105.455	105.032	N13-C14-C15-H22	-119.540	-119.719
C3-C4-H19	128.756	128.925	N13-C14-C15-H23	119.841	119.703
C5-C4-H19	125.789	126.043	O17-C14-C15-N11	-179.859	-179.952
O1-C5-C4	111.694	112.059	O17-C14-C15-H22	60.449	60.289
O1-C5-N6	117.530	117.591	O17-C14-C15-H23	-60.170	-60.290
C4-C5-N6	130.776	130.351	N13-H21-O39-C24	131.802	138.455
C5-N6-O7	115.962	118.311	O39-C24-C25-C26	121.712	121.182
C5-N6-O8	118.210	115.827	O39-C24-C25-H29	-110.637	-111.396
O7-N6-O8	125.828	125.862	O39-C24-C25-N38	7.145	6.465
C2-C9-N10	119.112	120.840	O40-C24-C25-C26	-58.424	-58.950
C2-C9-H20	116.425	115.223	O40-C24-C25-H29	69.228	68.473
N10-C9-H20	124.463	123.936	O40-C24-C25-N38	-172.991	-173.666
C9-N10-N11	119.183	119.203	C25-C24-O39-H21	-137.071	-142.480
N10-N11-C12	120.235	120.029	O40-C24-O39-H21	43.091	37.677
N10-N11-C15	128.075	128.357	C24-C25-C26-C27	-87.827	-88.487
C12-N11-C15	111.690	111.607	C24-C25-C26-H30	153.638	153.036
N11-C12-N13	106.290	106.310	C24-C25-C26-H31	33.920	33.346
N11-C12-O16	126.428	126.399	H29-C25-C26-C27	147.112	146.670
N13-C12-O16	127.283	127.291	H29-C25-C26-H30	28.577	28.192
C12-N13-C14	113.498	113.501	H29-C25-C26-H31	-91.142	-91.498
C12-N13-H21	119.854	119.566	N38-C25-C26-C27	27.701	27.434
C14-N13-H21	126.641	126.912	N38-C25-C26-H30	-90.834	-91.044
N13-C14-C15	106.230	106.239	N38-C25-C26-H31	149.448	149.266
N13-C14-O17	127.864	127.998	C24-C25-N38-C28	115.036	115.687
C15-C14-O17	125.907	125.763	C24-C25-N38-H36	-118.849	-118.337
N11-C15-C14	102.292	102.341	C24-C25-N38-H37	-2.960	-2.412
N11-C15-H22	112.350	112.401	C26-C25-N38-C28	-5.686	-5.149
N11-C15-H23	112.353	112.358	C26-C25-N38-H36	120.429	120.827
C14-C15-H22	110.268	110.230	C26-C25-N38-H37	-123.682	-123.248
C14-C15-H23	110.255	110.126	H29-C25-N38-C28	-127.779	-127.047
H22-C15-H23	109.168	109.221	H29-C25-N38-H36	-1.664	-1.072
N13-H21-O39	151.592	150.761	H29-C25-N38-H37	114.225	114.854
C25-C24-O39	112.442	112.629	C25-C26-C27-C28	-39.586	-39.682
C25-C24-O40	116.316	116.146	C25-C26-C27-H32	-160.383	-160.502
O39-C24-O40	131.241	131.225	C25-C26-C27-H33	78.373	78.170
C24-C25-C26	113.840	113.809	H30-C26-C27-C28	79.409	79.277
C24-C25-H29	108.653	108.580	H30-C26-C27-H32	-41.388	-41.544
C24-C25-N38	106.233	106.598	H30-C26-C27-H33	-162.632	-162.871
C26-C25-H29	113.586	113.477	H31-C26-C27-C28	-158.759	-158.919
C26-C25-N38	104.605	104.554	H31-C26-C27-H32	80.444	80.261
H29-C25-N38	109.549	109.481	H31-C26-C27-H33	-40.800	-41.067
C25-C26-C27	103.655	103.692	C26-C27-C28-H34	-80.173	-79.746
C25-C26-H30	111.056	111.030	C26-C27-C28-H35	153.966	154.439
C25-C26-H31	109.836	109.847	C26-C27-C28-N38	35.662	36.050
C27-C26-H30	110.388	110.332	H32-C27-C28-H34	41.810	42.254
C27-C26-H31	113.631	113.681	H32-C27-C28-H35	-84.051	-83.562
H30-C26-H31	108.257	108.241	H32-C27-C28-N38	157.646	158.049
C26-C27-C28	103.435	103.363	H33-C27-C28-H34	161.690	162.203
C26-C27-H32	113.229	113.260	H33-C27-C28-H35	35.829	36.388
C26-C27-H33	110.488	110.468	H33-C27-C28-N38	-82.475	-82.002

C28-C27-H32	111.468	111.512	C27-C28-N38-C25	-18.679	-19.264
C28-C27-H33	110.233	110.183	C27-C28-N38-H36	-145.518	-146.052
H32-C27-H33	107.965	108.024	C27-C28-N38-H37	92.572	92.716
C27-C28-H34	111.324	111.355	H34-C28-N38-C25	99.484	98.882
C27-C28-H35	115.376	115.522	H34-C28-N38-H36	-27.355	-27.906
C27-C28-N38	103.593	103.486	H34-C28-N38-H37	-149.266	-149.138
H34-C28-H35	109.708	109.568	H35-C28-N38-C25	-141.711	-142.441
H34-C28-N38	108.006	108.010	H35-C28-N38-H36	91.450	90.772
H35-C28-N38	108.401	108.467	H35-C28-N38-H37	-30.461	-30.460
C25-N38-C28	109.046	109.086			
C25-N38-H36	113.594	113.609			
C25-N38-H37	101.377	102.068			
C28-N38-H36	112.331	112.193			
C28-N38-H37	111.754	111.525			
H36-N38-H37	108.259	107.940			
H21-O39-C24	157.701	161.029			

Table S2 Band Assignment of observed FT-IR, FT-Raman spectra and theoretical harmonic vibrational wavenumbers (in cm^{-1}) of NTF.

Unscaled DFT	**Scaled DFT**	**IR**	**Raman**	**Ped Assignment (%contribution)**
3630	3447	3278	-	R2[υ(NH)] (100)
3279	3132	3149	3150	R1[υ(C4H)](96)
3248	3104	3110	3113	R1[υ(C3H)] (96)
3095	2965	2950	-	[υ(C9H)](99)
3076	2949	-	2952	R2[$\upsilon_{as}(CH_2)$](100)
3035	2911	2916	2918	R2[$\upsilon_{s}(CH_2)$](99)
1871	1831	1805	-	R2[υ(C12O)](65)+R2[υ(C14O)](14)+ R2[δ'ring](6)+R2[υ(NC12)](5)
1830	1791	1780	1775	R2[υ(C14O)](64)+R2[υ(C12O)](14) + R2[υ(NC14)](7)
1660	1630	1652	1609	[υ(CN10)](55)+ρ[C9H] (15)+ R1[υ(C2C9)](15)+R1[υ(C2C3)](6)
1602	1574	1598	1582	R1[υ(C4C5)](30)+R1[υ(C2C3)](15)+[υ(NO8)](11)+[υ(NO7)](9)+ [υ(C9N)](8)+ δin[C3H](6)+ρ[C5N](5)
1577	1551	1564	1564	[υ(NO8)] (41)+ [υ(NO7)](32)+R1[υ(C2C3)](9)
1526	1502	1517	1511	R1[υ(C4C5)](29)+R1[δring](13)+ R1[υ(C2C9)](12)+R1[υ(C2C3)](12)+R1[υ(C5N)](5)+ [υ(C9N)](5)
1484	1461	1475	1476	R2[δin[CH_2]](92)
1425	1404	1400	1429	R1[υ(C3C4)](17)+R1[υ(OC2)](15)+R1[υ(OC5)](12)+δin[C4H](10)+ R1[υ(C2C3)](6) +ρ[C9H] (6)+δin[C3H](5)+δin[C2OC](5)
1404	1384	1380	1379	ρ[C9H](12)+R2[υ(N11C12)](11)+ω[CC15N](8) +R1[υ(C2C3)](8)+R1[υ(C3C4)](7)+R2[υ(NN)](6) +δin[C3H](5)
1375	1356	-	-	R2[δin(NH)](36)+R2[υ(NC14)](17)+ρ[C9H](7)
1363	1345	1338	1349	ρ[C9H](22)+[υ(NO7)](19)+R1[υ(C5N)](14)+ [υ(NO8)](11)+ δsci[C5NO](10)+R1[υ(C3C4)](7)
1346	1329	1323	1325	ω[CC15N](21)+δin[N13CH](20)+R2[υ(C12N13)](13)+ R2[υ(N11C12)](10)+ρ[HC9](5)
1323	1306			R2[υ(NC14)](19)+R2[υ(C14C)](19)+ω[CC15N](16)+R2[δin[C=O17](10)+R2[υ(C12N13)](7)+ R2[δring](6)
1288	1272	-	-	R1[υ(C3C4)](28)+R1[υ(C2C9)](11)+R1[υ(OC2)](10)+[υ(NO7)](8)+δin[C3H](7)+ [υ(NO8)](6)+ρ[C9H](6)
1270	1255	1243	1258	R2[υ(NN)](26)+R2[υ(NC15)](13)+R1[υ(OC5)](10)+R1[υ(OC2)](8)+R2[δin[NN](6)+δin[C4H](5)+

				R1[δ'ring] (5)
1248	1233	1232	1232	R1[υ(OC5)](25)+R2[υ(NN)](16)+R1[δ'ring](10)+R1[υ(OC2)](9)+R1[υ(C5N)](8)+R2[υ(NC15)](5)+ R1[υ(C2C3)](5)
1209	1196	1206	1209	ω[CC15N](23)+R2[υ(NC12)](21) +R2[υ(NC15)] (21)+R2[υ(NC14)](5)
1192	1179			δin[C3H](31)+δin[C4H](21)+ R1[υ(C5N)](9)+R1[δ'ring](7)+ R1[υ(OC5)](5)+R1[υ(C2C9)](5)
1191	1178	1168	1169	γ[CC15N] (96)
1115	1104	1108	-	R2[υ(C12N13)](37)+ R2[υ(NC14)](17)+ δin[NC12O] (10) +R2[δin[NH](10) +R2[υ(NC15)](7)+R2[υ(C14C)] (5)
1038	1030	1016	-	R1[δin[C4H](38)+R1[δin[C3H](26)+R1[υ(C3C4)](24)
1014	1007	-	-	ρ[CC15N](71)+ δoop[C14O] (15) +R2[τring] (6)
1000	993	-	-	R1[υ(OC2)](44)+R1[δ'ring](13)+R1[υ(OC5)](9)+R1[υ(C2C9)](8)
986	979	976	978	R1[δring](42)+R1[υ(OC5)](11)+R1[υ(C4C5)](9)+R1[υ(C5N)](8)+R1[υ(OC2)](6)+R1[υ(C2C3)](5)
921	915	902	901	ω[C9H](54) +τ[C9N] (24)+δoop[C3H](6) +R1[δoop[C4H] (5)
904	899			R1[δoop[C4H] (60)+δoop[C3H](18)+R1[τring](12)+ω[C9H](5)
892	887			R2[υ(C14C)](54)+R2[υ(NC14)](18)+δin[N13CH](7)
879	874	871	869	R1[δ'ring](17)+R2[δin[NN](17)+δ[C9CN](14)+R2[υ(NC15)](12)+R2[δ'ring](9)+R2[υ(NN)](8)+ R2[υ(NC12)](7)
831	826	825		δsci[C5NO](59)+R1[δ'ring](17)+R1[δring](7)
811	807	807	811	δoop[C3H](69)+δoop[C4H] (19)
787	783	781	785	R2[υ(NC12)](22)+R1[δ'ring](15)+R1[δring](12)+R2[δ'ring](8)+R1[δ(C2C9)](7)+δin[NC12O](5)+ δsci[C5NO](5)
741	738	746	-	δoop[C=O16](70)+R2[τ'ring](13)+R2[τring](8)
738	736			δoop[C5N](66)+δoop[CN](15)+R1[τ'ring](10)
690	689	684	686	R2[δring](26)+R2[υ(NC15)](16)+δin[NC12O](11)+R2[δ'ring](10)+δin[NNC](10)+δin[OC14CN](6)+ R2[υ(C14C)](5)
688	686			R1[τ'ring](35)+δoop[C2C9](33)+R1[τring](24)
616	615	-	623	δin[OC14CN](18)+R2[δ'ring](15)+δin[NC12O](14)+R2[δring](11)+δin[NN](9)+R2[δin[NN](6)
608	607	-	-	δoop[C=O17](40)+δoop[NH](38)+R2[τring](12)+ρ[CC15N](7)
603	602	607	608	R2[δ'ring](25)+R2[δring](19)+R2[υ(C12N13)](10)+R1[υ(C2C9)](5)
594	593			R1[τring] (53)+R1[τ'ring](24)+δoop[CN](17)
554	554	582	571	δoop[NH](54)+R2[δoop(C=O17)(26)+ρ[CC15N](10)+γ[CC15N](5)
553	553	551	552	ρ[C5N](43)+δin[NC5OC](20)+δin[C2OC](10)+R1[υ(C4C5)] (5)
463	463	466	468	δin[NN](17)+δin[C2OC](15)+ρ[C5N](12)+R1[υ(C5N)](11)+R1[δring](6)+δ[C9CN](6)+ R2[δin[NN](5)+δin[NC12O](5)
442	442	443	-	R1[υ(C5N)](19)+R2[δin[C=O17](12)+δsci[C5NO](8)+δin[C=O16](7)+δin[C2OC](6)+δ[C9CN](6)+ R1[δ'ring] (5)+R2[υ(C12N13)](5)+R2[δring](5)
400	401	405	405	δin[C=O17](33)+R1[υ(C5N)](11)+R2[δin(C=O16)(10)+R2[υ(C12N13)](6)+R2[υ(C14C)](6)+R1[δring](5)+ R2[υ(NC15)] (5)
378	379	-	387	τ[C9N](28)+R1[τ'ring](17)+R1[τring](13)+δoop[C2C9](10)+ω[NC9C](9)+δoop[CN](8)+δoop[NN](6)
298	299	-	298	τ[NN] (41)+δoop[NN](20)+τ[C9C](12)+ R2[τ'ring](9)+τ[C9N] (8)
293	294	-	-	R2[δin[NN](18)+δin[C=O16](17)+R1[δin[C5N](13)+δin[C2OC](12)+ρ[C5N](7)+R2[υ(NC12)](6)+ R1[υ(C2C9)](6)
222	223	-	215	R1[δin[C5N](33)+ρ[C5N](17)+δ[C9CN](12)+R1[υ(C2C9)](6)+R1[δring] (5)
194	195	-	-	δoop[CN](56)+τ[NN](13)+τ[C9N](7)+δoop[C2C9](6)
179	180	-	189	R2[τ'ring] (77)+δoop[NN](16)
142	143	-	-	R2[τring] (54)+δoop[NH](36)
136	137	-	159	R2[δin[NN](30)+δin[NN](21)+R1[δin[C5N](18)+δin[C2OC](13)
121	121	-	-	R2[τring](34)+δoop[NH](21)+δoop[C2C9](10)+τ[C5N](10)+δoop[CN](9)+δoop[NN](5)
75	76	-	77	τ[C5N](42)+δoop[NN](32)+R2[τ'ring] (9)
51	51	-	-	δ[C9CN](36)+δin[C2OC](29)+R2[δin[NN](17)+δin[NN](6)+R1[δin[C5N](5)

44	44	-	-	δoop[NN](30)+τ[C5N](20)+τ[C9C](17)+R2[τ'ring](11)+ δoop[C2C9](8)
24	25	-	-	δoop[NN](37)+τ[C9C](20) +τ[NN](19)+τ[C9N](7)+R2[τring](5)

Table S3 Observed and calculated vibrational wavenumbers (in cm^{-1}) of FT-IR, FT-RAMAN spectra of LP

Unscaled DFT	Scaled DFT	IR	Raman	PED assignment (% contribution)
3567	3391	3211	-	R3[$\upsilon_{as}(NH_2)$](100)
3490	3322	3153	-	R3[$\upsilon_{s}(NH_2)$](100)
3132	3000	3053	3006	R3[$\upsilon_{as}(C28H_2)$](87)+ R3[$\upsilon_{as}(C27H_2)$](6)
3123	2991	3008	2983	R3[$\upsilon_{as}(C26H_2)$](90)
3116	2985			R3[υ(C25H)](91)+R3[$\upsilon_{as}(C26H_2)$](5)
3110	2980	2981	-	R3[$\upsilon_{s}(C27H_2)$](82)+R3[$\upsilon_{s}(C28H_2)$](10)
3072	2945	2952	2950	R3[$\upsilon_{s}(C28H_2)$](95)
3065	2938	2910	2933	R3[$\upsilon_{s}(C27H_2)$](96)
3030	2907	2877	2874	R3[$\upsilon_{s}(C26H_2)$](97)
1764	1729	1614	1625	R3[υ(CO40)](60)+R3[υ(CO39)](28)+R3[δsci(C24CO)](8)
1576	1549	1554	1549	R3[δin(NH_2)](87)+R3[ω(NH_2)](5)
1513	1489	-	-	R3[δ($C28H_2$)](54)+R3[δ($C26H_2$)](24)+R3[δ($C27H_2$)](15)
1501	1478	1473	1472	R3[δ($C28H_2$)](40)+R3[δ($C27H_2$)](36)+R3[δ($C27H_2$)](21)
1494	1471	1448	1453	R3[δ($C27H_2$)](60)+R3[δ($C26H_2$)](37)
1388	1368	1375	1375	R3[ω($C28H_2$)](61)+R3[υ(C27C28)](7)+R3[ω(NH_2)](7) +R3[ω($C26H_2$)](7)+R3[γ(NH_2)](6)
1361	1342	-	1349	R3[ω($C27H_2$)](38)+R3[ω($C26H_2$)](14)+R3[γ($C27H_2$)](11)+R3[υ(C26 C27)](8)+R3[γ($C26H_2$)](8)+R3[γ($C28H_2$)](7)
1350	1332	-	-	R3[δ(NC25C26)](19)+R3[ω($C27H_2$)](10)+R3[ω($C28H_2$)](10)+R3[ω(NH_2)](8)+R3[υ(CO39)](8)+R3[ω($C26H_2$)](7)+R3[υ(C25C)](6) +R3[γ($C27H_2$)](6)+R3[γ(NH_2)](5)
1327	1310	1319	1316	R3[ω($C26H_2$)](22)+R3[δ(NC25C26)](20)+R3[ω($C27H_2$)](16)+ R3[γ(NH_2)](11)+R3[υ(CO39)](9)
1318	1301	1292	1286	R3[υ(CO39)](21)+[ω($C26H_2$)](13)+R3[υ(CO40)](12)+ R3[γ($C28H_2$)](11)+R3[ω($C27H_2$)](6)+R3[δoop(C25H)](5)+ R3[ω(NH_2)](5)+R3[δ(NC25C26)](5)+R3[ω($C28H_2$)](5)
1288	1272	-	1266	R3[υ(CO39)](14)+R3[γ($C28H_2$)](12)+R3[δoop(C25H)](11)+ R3[γ($C26H_2$)](10)+R3[υ(C24C)]+(9)+R3[υ(C25C)](8) +R3[ω($C26H_2$)](6)+[γ($C4H_2$)](6)+[ω(C2NC)](5)
1278	1263	-	-	R3[δoop(C25H)](31)+R3[γ(C27CN)](29)+R3[γ(C27C)](7) +R3[ρ($C26H_2$)](6)
1263	1248	1253	1238	R3[δ(NC25C26)](23)+R3[γ(NH_2)](18)+R3[γ($C26H_2$)](9) +R3[ρ($C28H_2$)](8)+R3[ρ($C27H_2$)](8)+R3[ω($C28H_2$)](6)
1211	1197	-	-	R3[ω(NH_2)](40)+R3[γ($C27H_2$)](16)+R3[ω($C28H_2$)](8) +R3[ω($C27H_2$)](5)+R3[υ(C27C28)](5)
1190	1177	1168	1175	R3[γ($C26H_2$)](23)+R3[υ(C26C27)](11)+R3[υ(C26C27)](10) +R3[ω($C27H_2$)](8)+R3[γ($C27H_2$)](7)+R3[ω(NH_2)](6) +R3[δ(NC25C26)](6)+R3[ρ($C28H_2$)](5)

1133	1122	-	-	R3[δoop(C25H)](32)+R3[γ(NH_2)](27)+R3[γ($C27H_2$)](8)
1090	1080	1083	1083	R3[ρ($C26H_2$)](18)+R3[γ($C26H_2$)](18)+R3[ρ($C28H_2$)](11) +R3[δ(NC25C26)](10)+ R3[υ(C25C)](8)+R3[ρ($C27H_2$)](7)+R3[υ(C25N)](5)
1039	1030	1033	1033	R3[υ(C4C5)](20)+R3[υ(C26C27)](14)+R3[υ(C25C)](11)+ R3[δring](10)+R3[γ(NH_2)](6)+R3[ω($C26H_2$)](5)+R3[ω($C27H_2$)](5)+ R3[ρ($C26H_2$)](5)+R3[υ(C28N)](5)
1014	1006	981	985	R3[υ(C28N)](23)+R3[ρ($C27H_2$)](14)+R3[υ(C25C)](12) +R3[δ'ring](11)+R3[υ(C25N)](9)+R3[υ(C27C28)](8)+R3[γ(NH_2)](6) +R3[δring](6)
955	949	946	951	R3[ρ($C26H_2$)](15)+R3[δoop(C25C24)](13)+R3[ρ($C28H_2$)](12) +R3[γ($C28H_2$)](11)+R3[ρ(NH_2)](10)+R3[γ($C27H_2$)](8) +R3[υ(C25C)](6)+R3[γ($C26H_2$)](5)
935	929	-	920	R3[υ(C28N)](16)+R3[υ(C26C27)](15)+R3[υ(C25C)](13) +R3[υ(C24C)](9)+R3[γ($C27H_2$)](8)+R3[ρ(NH_2)](6)
909	904	902	898	R3[υ(C27C28)](43)+R3[υ(C26C27)](33)+R3[υ(C5N)](7)
889	884	860	866	R3[υ(C28N)](29)+R3[ρ($C26H_2$)](11)+R3[ρ($C27H_2$)](10) +R3[υ(C25N)](6)
845	840	846	842	R3[υ(C25N)](19)+R3[ρ($C28H_2$)](19)+R3[ρ($C27H_2$)](14)+ R3[δsci(C24CO)](8)+R3[υ(C28N)](8)+R3[υ(C26C27)](6)
819	815			R3[υ(C24C)](26)+R3[δsci(C24CO)](17)+R3[ρ(C24CO)](17)+ R3[υ(C25N)](9)+R3[ρ($C26H_2$)](8)
790	787	694	-	R3[υ(C25N)](41)+R3[ρ(C24CO)](19)+R3[ρ(NH_2)](11)
764	761	-	-	R3[δoop(C24C)](41)+R3[ρ(NH_2)](22)+R3[δoop(C25H)](10)+ R3[δoop(C25C24)](8)+R3[ρ($C27H_2$)](6)+R3[δ(NC25C26)](5)
653	652	640	642	R3[δring](44)+R3[δ'ring](9)+R3[ρ($C28H_2$)](7)+R3[δoop(C24C)](7)+ R3[ρ(C24CO)](6)+R3[ρ($C26H_2$)](6)+R3[ρ(NH_2)](5)
604	603	-	-	R3[υ(C24C)](30)+R3[δsci(C24CO)](29)+R3[δoop(C24C)](11)+ R3[δoop(C25C24)](10)+R3[υ(C25C)](7)
576	576	570	573	R3[δ'ring](42)+R3[ρ($C27H_2$)](18)+R3[ρ($C26H_2$)](8)+R3[δring](7) +R3[ρ($C28H_2$)](7)
464	465	449	448	R3[δsci(C24CO)](18)+R3[δ(NC25C26)](17)+R3[υ(C24C)](16) +R3[ρ(C24CO)](16) +R3[υ(C25N)](8)+R3[δring](6) +R3[δoop(C24C)](5)
315	317		296	R3[δoop(C25C24)](42)+R3[δoop(C25H)](7)+R3[τ'_{ring}](7)+R3[τ_{ring}](6)+R3[δoop(C24C)](6)+R3[ρ(NH_2)](5)
272	274			R3[δ(NC25C26)](27)+R3[ρ(C24CO)](15)+R3[δsci(C24CO)](13)+R3[ρ(NH_2)](9)+R3[τ_{ring}](8)+R3[υ(NH_2)](7)
184	185		160	R3[τ_{ring}](33)+R3[δoop(C25C24)](27)+R3[δ(NC25C26)](22)
140	141		136	R3[ρ(C25NC)](30)+R3[τ_{ring}](21)+R3[τ'_{ring}](17)+ R3[δoop(C25C24)](8)+R3[υ(NH_2)](5)
119	120		122	[τ(C24C)](48)+R3[τ'_{ring}](12)+R3[δoop(C25C24)](12)+R3[δ(NH_2)](6) +R3[δ(NC25C26)](6)+R3[ω(NH_2)](5)

Table S4 AIM calculation to determine characteristics (bond length (Å), Angles (°)) of hydrogen bonds and ellipticity index (ε) around bond critical point (BCP) of NTF-LP cocrystal

Interactions (D-H···A)	d_{D-H}(Å)	$d_{H\cdots A}$(Å)	d_{D-A}(Å)	D-H···A( )	r_H+r_A(Å)	ε
N13-H21···O39	1.03854	1.70992	2.66953	151.59237	2.72	2.7826×10^{-2}
N38-H37···O39	1.05855	1.74201	2.51021	125.58419	2.72	5.9416×10^{-2}
N38-H37···O16	1.05855	2.24165	3.02014	128.83140	2.72	20.4821×10^{-2}
C28-H35···O16	1.08811	2.55865	3.26643	121.85679	2.72	47.7837×10^{-2}

Table S5 Selective local reactive descriptors of interacting atoms of NTF (API) explaining their reactive sites.

Atoms	f_k^o	s_k^o	w_k^o	Atoms	f_k^+	s_k^+	w_k^+	Atoms	f_k^-	s_k^-	w_k^-
1O	–0.2756	–0.0278	–0.5569	1O	0.0679	0.0068	0.1372	1O	0.0426	0.0043	0.0862
2O	–0.2760	–0.0278	–0.5577	2O	0.0563	0.0057	0.1137	2O	0.0426	0.0043	0.0861
3O	–0.0743	–0.0075	–0.1501	3O	0.0234	0.0024	0.0473	3O	0.0352	0.0035	0.0712
4O	–0.2261	–0.0228	–0.4569	4O	0.0513	0.0052	0.1036	4O	0.1221	0.0123	0.2467
5O	–0.2433	–0.0245	–0.4916	5O	0.0622	0.0063	0.1257	5O	0.1268	0.0128	0.2563
6N	–0.0770	–0.0078	–0.1556	6N	0.0260	0.0026	0.0525	6N	0.0137	0.0014	0.0277
7N	0.0329	0.0033	0.0666	7N	0.0869	0.0087	0.1755	7N	0.0152	0.0015	0.0306
8N	–0.0785	–0.0079	–0.1585	8N	0.0576	0.0058	0.1164	8N	0.0722	0.0073	0.1459
9N	0.2111	0.0213	0.4266	9N	0.0144	0.0014	0.0291	9N	0.0680	0.0068	0.1374
10C	0.2155	0.0217	0.4355	10C	0.0268	0.0027	0.0541	10C	0.0311	0.0031	0.0628
11C	0.1907	0.0192	0.3853	11C	0.0143	0.0014	0.0289	11C	0.0169	0.0017	0.0341
12C	0.0094	0.0009	0.0190	12C	0.0182	0.0018	0.0367	12C	0.0093	0.0009	0.0188
13C	0.0255	0.0026	0.0515	13C	0.0634	0.0064	0.1280	13C	0.0570	0.0057	0.1151
14C	0.0674	0.0068	0.1362	14C	0.0506	0.0051	0.1022	14C	0.0523	0.0053	0.1058
15C	0.1183	0.0119	0.2390	15C	0.0807	0.0081	0.1631	15C	0.0413	0.0042	0.0835
16C	–0.0499	–0.0050	–0.1008	16C	0.0509	0.0051	0.1029	16C	0.0656	0.0066	0.1326
17C	–0.0407	–0.0041	–0.0822	17C	0.0823	0.0083	0.1662	17C	0.0506	0.0051	0.1022
18H	0.1688	0.0170	0.3411	18H	0.0243	0.0024	0.0490	18H	0.0178	0.0018	0.0359
19H	0.0649	0.0065	0.1312	19H	0.0246	0.0025	0.0497	19H	0.0112	0.0011	0.0227
20H	0.0649	0.0065	0.1312	20H	0.0246	0.0025	0.0497	20H	0.0112	0.0011	0.0227
21H	0.0417	0.0042	0.0842	21H	0.0270	0.0027	0.0546	21H	0.0299	0.0030	0.0605
22H	0.0684	0.0069	0.1381	22H	0.0309	0.0031	0.0625	22H	0.0353	0.0036	0.0714
23H	0.0620	0.0062	0.1254	23H	0.0357	0.0036	0.0721	23H	0.0319	0.0032	0.0644

Table S6 Selective local reactive descriptors of interacting atoms of LP explaining their reactive sites.

Atoms	f_k^o	s_k^o	w_k^o	Atoms	f_k^+	s_k^+	w_k^+	Atoms	f_k^-	s_k^-	w_k^-
1C	0.1852	0.0384	0.5346	1C	0.1048	0.0217	0.3025	1C	0.0135	0.0028	0.0390
2C	0.0443	0.0092	0.1280	2C	0.0583	0.0121	0.1682	2C	0.0257	0.0053	0.0741
3C	–0.0507	–0.0105	–0.1463	3C	0.0186	0.0038	0.0536	3C	0.0249	0.0052	0.0719
4C	–0.0496	–0.0103	–0.1430	4C	0.0142	0.0029	0.0409	4C	0.0284	0.0059	0.0818
5C	0.0002	0.0001	0.0007	5C	0.0184	0.0038	0.0532	5C	0.0794	0.0165	0.2292
6H	0.0350	0.0073	0.1011	6H	0.0380	0.0079	0.1096	6H	0.0626	0.0130	0.1807
7H	0.0177	0.0037	0.0510	7H	0.0362	0.0075	0.1046	7H	0.0619	0.0128	0.1788
8H	0.0491	0.0102	0.1416	8H	0.0144	0.0030	0.0416	8H	0.0221	0.0046	0.0639
9H	0.0274	0.0057	0.0791	9H	0.0279	0.0058	0.0804	9H	0.0637	0.0132	0.1838
10H	0.0409	0.0085	0.1180	10H	0.0076	0.0016	0.0219	10H	0.0208	0.0043	0.0600
11H	–0.0276	–0.0057	–0.0797	11H	0.0227	0.0047	0.0656	11H	0.1697	0.0352	0.4899

12H	0.0272	0.0056	0.0786	12H	0.0237	0.0049	0.0685	12H	0.0768	0.0159	0.2215
13H	0.0521	0.0108	0.1503	13H	0.0303	0.0063	0.0876	13H	0.2493	0.0516	0.7194
14H	0.1110	0.0230	0.3204	14H	0.0235	0.0049	0.0679	14H	0.0295	0.0061	0.0851
15N	0.0157	0.0033	0.0453	15N	0.0250	0.0052	0.0723	15N	0.0132	0.0027	0.0382
16O	–0.2885	–0.0598	–0.8327	16O	0.1480	0.0307	0.4270	16O	0.0195	0.0040	0.0562
17O	–0.1856	–0.0384	–0.5355	17O	0.3883	0.0804	1.1205	17O	0.0310	0.0064	0.0894